

Spinodal decomposition in an order-disorder phase transition with elastic fields

Celeste Sagui,¹ A. M. Somoza,² and Rashmi C. Desai¹

¹*Department of Physics, University of Toronto, Toronto, Ontario, Canada M5S 1A7*

²*Instituto de Ciencia de Materiales, Consejo Superior de Investigaciones Científicas, Universidad Autónoma (C-XII), Madrid E-28049, Spain*

(Received 20 July 1994)

We study the effect of an elastic field in an order-disorder phase transition described by the dynamics corresponding to a model C system. The elastic field is coupled to both the concentration and the order parameter. By assuming that the elastic field relaxes very fast, we express it in terms of the conserved variable and the order parameter. We concentrate our study on the long-range Eshelby interaction that arises due to the difference of shear moduli in the ordered and disordered phases. This elastic interaction modifies dramatically the spinodal decomposition, by changing the morphology of domains and slowing their growth (which in the absence of an elastic field varies as $t^{1/3}$). Changes in morphology are more dramatic when there are competing effects between the wetting regime of model C and the elastic energy. The elastic misfits create an energy barrier of soft phase around the hard phase precipitates. This energy barrier leads the system to very sluggish growth and to an eventual frozen metastable state.

PACS number(s): 61.50.Ks, 64.75.+g, 81.30.-t, 81.40.Jj

I. INTRODUCTION

During phase separation of alloys, elastic fields originate from the elastic misfit or the difference in the lattice constant of the phases [1]. These long-range fields can drastically influence the domain morphology. In particular, the elastic anisotropy of crystals or the anisotropy brought about by external stresses gives rise to modulated structures with nearly periodic patterns in late-stage spinodal decomposition [2]. It has been observed experimentally that the growth of modulated structures is characterized by an exponent that depends on the composition of the alloy. Also, for alloys with large lattice misfits, the coarsening rate becomes extremely slow, and in many cases the precipitates become stable against coarsening and growth stops [3].

Ardell *et al.* [2] studied experimentally a cuboidal modulated structure; Eshelby in an Appendix to this paper calculated a pairwise interaction among spherical precipitates when the elastic moduli are different (Eshelby's interaction). Khachatryan presented a study of structural transitions for nonconserved order parameters [1]. Cahn studied the effects of elastic fields on phase transitions with conserved order parameter [4]. Kawasaki and Enomoto [5] investigated the Eshelby interaction for spherical domains in Ostwald ripening at small volume fractions. Johnson and Voorhees [6] studied the elastically induced concentration changes in two-phase systems and found that elastic misfit strains affect the equilibrium solute distribution.

Recently, Onuki and Nishimori [7] have presented a Ginzburg-Landau approach to analyze the elastic effects in phase-separating alloys in a model B system. In their work, the authors consider the so-called coherent case in which precipitates have lattice constants that are different from that of the matrix and the lattice planes are

continuous through the two-phase region. They assume that the elastic strain is a subsidiary tensor variable coupled to a conserved order parameter, the concentration. By further assuming that the elastic field relaxes very fast with respect to the concentration, they obtained an effective energy to describe the interactions among the concentration fluctuations when the elastic moduli weakly depend on the concentration.

Model B contains the essential physics for some simple systems, but generally, many alloys undergo order-disorder transitions in which the nonconserved order parameter related to the symmetry of the alloy is coupled to the conserved variable (the concentration). For such systems, the description given by model B is inadequate since we need two coupled differential equations, as described in the simplest case by model C.

For a model A system, a quench from the disordered phase into the ordered phase induces a symmetry-breaking transition and the nonconserved order parameter reflects the degree of local ordering in the system. For a model B system, the conserved order parameter is proportional to a density or concentration, and reflects the extent of the phase separation in the system. Typically, an initial mixed state is quenched inside the coexistence region, where it separates into two or more phases. In this case, all the phases involved have the same symmetry, including the initial mixed one. For both model A and model B, the disordered state is a stable minimum of the bulk free energy density before the quench, and an unstable maximum after the quench. In contrast to this situation, a quench for a model C system from the disordered state into the coexistence region of a symmetry-breaking, first-order phase transition shows three minima at the final temperature: the minimum corresponding to the disordered phase coexists with the degenerate minima corresponding to the two ordered states of the non-

conserved order parameter.

Order-disorder transitions are common in binary alloys. The order-disorder transitions in the Fe-rich Fe-Al alloys were first reported in 1932 by Bradley and Jay [8]. Since that time, much effort has been put into understanding order-disorder transitions in general. Allen and Cahn [9] have studied the coherent and incoherent equilibria in iron-rich iron-aluminum alloys, as well as the mechanisms of phase transformations within the miscibility gap of these alloys. The phase diagram has a disordered phase, α , and two ordered phases, FeAl and Fe₃Al. The transitions $\alpha \rightarrow$ FeAl and FeAl \rightarrow Fe₃Al are second-order transitions. Here we will look at the part of the phase diagram that involves the α phase (disordered bcc) and the FeAl phase (ordered bcc). The $\alpha \rightarrow$ FeAl second-order transition line is usually known as the “ λ -line” and ends in a symmetrical tricritical point; below this point the transition is first order. Allen and Cahn showed the importance of elastic effects in these alloys, and the existence of an equilibrium incoherent phase diagram and a coherent metastable phase diagram (see Fig. 1).

Recently, we have studied the spinodal decomposition in an order-disorder phase transition described by model C [10]. In this work we showed how the wetting properties of the disordered phase can alter the morphology of the domains after the quench. The purpose of the present paper is to study the effect of an elastic field in order-disorder phase transitions. We study a model C system and couple the elastic field to both the concentration and the order parameter. We choose the parameters of the free energy such that in absence of elastic fields the disordered phase completely wets the ordered phase. In our system, the elastic field cannot distinguish between the two ordered states but can certainly distinguish between

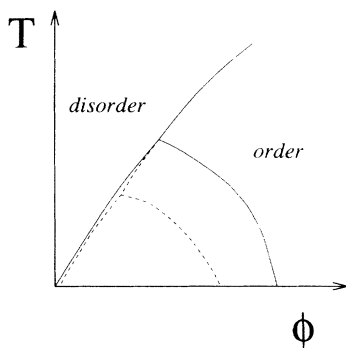


FIG. 1. Sketch of the temperature-concentration phase diagram. The solid lines correspond to the incoherent stable state and the dashed lines to the coherent metastable state. If this sketch were to represent part of the phase diagram of an Fe-rich Fe-Al alloy, the *disordered* phase would correspond to the α phase (disordered bcc) and the ordered phase to FeAl (ordered bcc). These phases are separated by a line of second-order transitions (the λ line) which ends at the miscibility gap between the same phases. The point where the λ -transition line meets the two first-order coexistence lines is a tricritical point. The elastic effects in the coherent phase diagram have lowered this tricritical point.

the degenerate ordered minima and the disordered minimum. This means that in the coarse-grained free energy that describes the system, the coupling term between the elastic field and the nonconserved order parameter must be an even function of the order parameter. In Sec. II we present the model for constant elastic moduli and for elastic moduli that vary with the concentration and the order parameter. In Sec. III we describe our simulations and present the results. In Sec. IV we give the conclusions of our study. We have also included an Appendix where we derive the interface equations.

II. MODEL

A. Constant elastic moduli

In this section we introduce the coarse-grained Ginzburg-Landau free energy functional that corresponds to a model C system and study the effect of coupling an elastic field. We call ϕ the conserved variable and ψ the symmetry related scalar order parameter. The elastic strain $\mu_{ij} = \frac{1}{2}(\frac{\partial u_i}{\partial x_j} + \frac{\partial u_j}{\partial x_i})$ is a subsidiary tensor variable coupled to both ϕ and ψ . We assume the coherent condition at the interface, i.e., the lattice planes are continuous through the interface. In this subsection we assume that the system is isotropic and that the elastic moduli are constants. The condition of mechanical equilibrium allows us to express the elastic field in terms of the conserved variable and the order parameter. The only contribution of the isotropic elastic terms with constant elastic moduli is to renormalize the coefficients of the free energy, or equivalently, to displace the coexistence and spinodal lines in the phase diagram. Thus we can obtain a dimensionless expression of the free energy where all these effects have been absorbed. In the next subsection we generalize our treatment to the case where the elastic coefficients depend on ϕ and ψ .

The coarse-grained Ginzburg-Landau free energy is

$$F[\phi, \psi, \mu] = \int d\mathbf{r} \left[\frac{l_\psi^2}{2} [\nabla\psi(\mathbf{r})]^2 + \frac{l_\phi^2}{2} [\nabla\phi(\mathbf{r})]^2 + \tilde{f}(\phi, \psi, \mu) \right]. \quad (1)$$

The bulk free energy density $\tilde{f}(\phi, \psi, \mu)$ is

$$\tilde{f}(\phi, \psi, \mu) = \frac{1}{2}r\psi^2 + u\psi^4 + v\psi^6 + \frac{1}{2}\chi_n^{-1}\phi^2 + \gamma\phi\psi^2 - \Delta\phi + \epsilon_\phi\phi\nabla \cdot \mathbf{u} + \epsilon_\psi\psi^2\nabla \cdot \mathbf{u} + \tilde{f}_{el}(\mu), \quad (2)$$

where $\nabla \cdot \mathbf{u}$ is the trace of the strain tensor μ and ϵ_ϕ and ϵ_ψ are constants that, respectively, couple $\nabla \cdot \mathbf{u}$ to the conserved variable and the order parameter. \tilde{f}_{el} is the isotropic elastic energy for a d -dimensional system given by

$$\tilde{f}_{el}(\mu) = \frac{1}{2}\kappa'_0(\nabla \cdot \mathbf{u})^2 + \mu'_0 \sum_{i,j} \left(\mu_{ij} - \frac{\delta_{ij}}{d} \nabla \cdot \mathbf{u} \right)^2. \quad (3)$$

Here κ'_0 and μ'_0 are the bulk and shear elastic moduli [11]. We assume for simplicity that the parameters r , u , v , γ , χ_n , ϵ_ϕ , ϵ_ψ , κ'_0 and μ'_0 depend only on the temperature T . Considerations of stability require v , χ_n , κ'_0 and μ'_0 all greater than zero. Δ is the chemical potential associated with the alloy.

If we set $\mu_{ij} = 0$ we are left with the model used by several authors [12] to describe tricritical systems in alloys and in superfluid ^3He - ^4He mixtures (where the order parameter is complex). Minimizing the free energy density (without elastic fields) with respect to ϕ with ψ fixed gives $\phi = \chi_n(\Delta - \gamma\psi^2)$ and substitution in Eq. (2) with $\mathbf{u} = 0$ gives $f_{tric}(\psi) = \frac{1}{2}\tilde{r}\psi^2 + \tilde{u}\psi^4 + v\psi^6 + \frac{1}{2}\chi_n\Delta^2$, where $\tilde{r} = r + 2\Delta\gamma\chi_n$ and $\tilde{u} = u - \frac{1}{2}\gamma^2\chi_n$. Thus a mean-field analysis shows that there is a line of second-order phase transitions for $\tilde{r} = 0$ and $\tilde{u} > 0$. For negative \tilde{u} , there is a line of first-order transitions at $\tilde{r} = \tilde{u}^2/(2v)$ with a tricritical point at $\tilde{r} = 0, \tilde{u} = 0$. On the disordered side of the first-order line, $\psi^2 = 0$ and $\phi = \chi_n\Delta$, while on the ordered side of the first-order line $\psi^2 = \psi_s^2 = |\tilde{u}|/(2v)$ and $\phi_s = \chi_n\Delta - \gamma\chi_n|\tilde{u}|/(2v)$.

The mean-field approximation to the free energy is obtained by minimizing the integrand with respect to the components of the displacement vector \mathbf{u} , ϕ and ψ for fixed T and Δ . The stress is defined as

$$\sigma_{ij} = \frac{\partial F}{\partial \mu_{ij}}, \quad (4)$$

$$\begin{aligned} \sigma_{ij} &= (\epsilon_\phi\phi + \epsilon_\psi\psi^2 + \kappa'_0\nabla \cdot \mathbf{u})\delta_{ij} \\ &+ 2\mu'_0 \left(\mu_{ij} - \frac{\delta_{ij}}{d} \nabla \cdot \mathbf{u} \right). \end{aligned} \quad (5)$$

The mechanical equilibrium condition requires that

$$\frac{\delta F}{\delta \mathbf{u}_i} = \sum_j \frac{\partial \sigma_{ij}}{\partial x_j} = 0, \quad (6)$$

which translates into

$$\begin{aligned} \left[\kappa'_0 + \left(1 - \frac{2}{d} \right) \mu'_0 \right] \nabla \nabla \cdot \mathbf{u} + \epsilon_\phi \nabla \phi + \epsilon_\psi \nabla \psi^2 \\ + \mu'_0 \nabla^2 \mathbf{u} = 0. \end{aligned} \quad (7)$$

The solution of this equation is

$$\nabla \cdot \mathbf{u} = \text{Tr} A - \frac{1}{k'_{10}} (\epsilon_\phi \bar{\phi} + \epsilon_\psi \psi^2), \quad (8)$$

where we have assumed a constant external strain A_{ij} , $\bar{\phi} = \phi - \phi_0$ with ϕ_0 as the concentration before the quench, and $k'_{10} = \kappa'_0 + 2\mu'_0(1 - 1/d)$. In absence of external strain, this equation coincides with that obtained by Allen and Cahn [9] (they only consider the compression-dilation term, i.e., $\mu'_0 = 0$ and $k'_{10} = \kappa'_0$) and its interpretation is the following. The lattice constant a changes

both as a function of ϕ and ψ . If we consider a along the x direction, we can write $a = a_0(1 + \partial u_x/\partial x)$ and the relative change in volume of the system after the quench is

$$\frac{\delta V}{V} = \nabla \cdot \mathbf{u} = -\frac{1}{k'_{10}} (\epsilon_\phi \bar{\phi} + \epsilon_\psi \psi^2). \quad (9)$$

If we substitute the expression for $\nabla \cdot \mathbf{u}$ in Eq. (7), we find

$$\frac{\partial u_i}{\partial x_j} = A_{ij} - \frac{\epsilon_\phi}{k'_{10}} \frac{\partial^2 W_\phi}{\partial x_j \partial x_i} - \frac{\epsilon_\psi}{k'_{10}} \frac{\partial^2 W_\psi}{\partial x_j \partial x_i}, \quad (10)$$

with

$$\nabla^2 W_\phi = \phi - \phi_0 = \bar{\phi} \quad \text{or} \quad W_\phi = \frac{1}{\nabla^2} \bar{\phi},$$

and

$$\nabla^2 W_\psi = \psi^2 \quad \text{or} \quad W_\psi = \frac{1}{\nabla^2} \psi^2. \quad (11)$$

This expresses the strain tensor in terms of the order parameters ϕ and ψ . If we substitute Eq. (10) with $A_{ij} = 0$ in Eq. (2) we find that the contribution of the elastic terms renormalizes the coefficients of the free energy density, which now reads

$$\begin{aligned} \tilde{f}(\phi, \psi) &= \frac{1}{2} r \psi^2 + \left(u - \frac{\epsilon_\psi^2}{2k'_{10}} \right) \psi^4 + v \psi^6 \\ &+ \frac{1}{2} \left(\chi_n^{-1} - \frac{\epsilon_\phi^2}{2k'_{10}} \right) \phi^2 \\ &+ \left(\gamma - \frac{1}{k'_{10}} \epsilon_\psi \epsilon_\phi \right) \phi \psi^2 - \Delta \phi + \frac{\epsilon_\psi^2 \phi_0^2}{2k'_{10}}. \end{aligned} \quad (12)$$

This has the same form as the energy for the model C system without elastic fields, except that some parameters have been renormalized:

$$\begin{aligned} u_1 &= u - \frac{\epsilon_\psi^2}{2k'_{10}}, \\ \chi_{n1}^{-1} &= \chi_n^{-1} - \frac{\epsilon_\phi^2}{2k'_{10}}, \\ \gamma_1 &= \gamma - \frac{1}{k'_{10}} \epsilon_\psi \epsilon_\phi. \end{aligned} \quad (13)$$

These parameters reduce to the ones of the simple model C system when the coupling constants ϵ_ϕ and ϵ_ψ go to zero. Now we can repeat the analysis done for the incoherent tricritical system and find

$$\begin{aligned} \tilde{r}_1 &= r + 2\Delta\gamma_1\chi_{n1} = r + 2\Delta\chi_n \left(\frac{\gamma k'_{10} - \epsilon_\psi \epsilon_\phi}{k'_{10} - \chi_n \epsilon_\phi^2} \right), \\ \tilde{u}_1 &= u - \frac{1}{2} \gamma_1^2 \chi_{n1} - \frac{\epsilon_\psi^2}{2k'_{10}} \\ &= u - \frac{1}{2} \frac{k'_{10} \chi_n}{(k'_{10} - \chi_n \epsilon_\phi^2)} \left(\gamma - \frac{\epsilon_\psi \epsilon_\phi}{k'_{10}} \right) - \frac{\epsilon_\psi^2}{2k'_{10}}, \\ \phi &= \chi_{n1} \Delta - \gamma_1 \chi_{n1} \psi^2 \\ &= \frac{\chi_n}{(k'_{10} - \chi_n \epsilon_\phi^2)} \left[k'_{10} \Delta - (\gamma k'_{10} - \epsilon_\psi \epsilon_\phi) \psi^2 \right]. \end{aligned} \quad (14)$$

For $\tilde{u}_1 > 0$, there is a line of second-order phase transitions at $\tilde{r}_1 = 0$. For $\tilde{u}_1 < 0$, there is a line of first-order transitions at $\tilde{r}_1 = \tilde{u}_1^2/(2v)$ with a coherent tricritical point at $\tilde{r}_1 = 0, \tilde{u}_1 = 0$. The value of ψ on the disordered side of the first-order line is $\psi^2 = 0$ as before, and on the ordered side is $\psi^2 = \psi_{s1}^2 = |\tilde{u}_1|/(2v)$ while the values of the concentration are $\phi_{n1} = \chi_{n1}\Delta$ and $\phi_{s1} = \chi_{n1}\Delta - \gamma_1\chi_{n1}|\tilde{u}_1|/(2v)$. A linear analysis shows the new spinodal lines:

$$\phi_1 = -\frac{r}{2\gamma_1}, \quad (15)$$

$$\phi_2 = -\frac{r}{2\gamma_1} + \frac{\tilde{u}_1}{3\gamma_1 v} \left[u_1 + \frac{\chi_{n1}\gamma_1^2}{2} \right].$$

ϕ_1 is the spinodal line near the disordered side of the coexistence line and ϕ_2 is that near the ordered side. If $\tilde{f}_{adiab}(\phi)$ is the adiabatic approximation of $\tilde{f}(\phi, \psi)$ (obtained by replacing ψ as a function of ϕ) then $\partial^2 \tilde{f}_{adiab}(\phi)/\partial\phi^2$ has a jump discontinuity at $\phi = \phi_1$ going from positive for $\phi > \phi_1$ to negative for $\phi < \phi_1$, while it goes continuously to zero at $\phi = \phi_2$. We define the temperature coefficient of $f_{\phi\phi} = \partial^2 \tilde{f}_{adiab}(\phi)/\partial\phi^2$ along the λ curve as $f_{\phi\phi T} = \partial f_{\phi\phi}/\partial T$ [9]. Then one can compute the temperature difference between the incoherent and coherent tricritical point as $T^{incoh} - T^{coh} = \frac{1}{f_{\phi\phi T}}(f_{\phi\phi}^{incoh} - f_{\phi\phi}^{coh})$.

Figure 1 shows the phase diagram for the coherent and incoherent case. If the elastic field is isotropic and the elastic coefficients are constants, the only effect of coupling an elastic field to the order parameter and concentration is just to switch the positions of the lines of the phase diagram, but this effect can be absorbed by renormalizing the coefficients of the free energy, such that the functional form of the coherent free energy is the same as that of the incoherent one. In particular, it is always possible to rescale the relevant quantities to obtain dimensionless equations.

We want to study a quench into the unstable region of the phase diagram, where coexistence fixes the value of Δ : $\Delta = \Delta_0$ for $\tilde{r}_1 = \tilde{u}_1^2/(2v)$. It is possible to rescale the units of energy, concentration, and order parameter. We introduce the dimensionless order parameter y and the dimensionless concentration c :

$$-\frac{\tilde{u}_1}{2v}y^2 = \psi^2, \quad (16)$$

$$\phi = \chi_{n1}\Delta_0 + \gamma_1\chi_{n1}\frac{|\tilde{u}_1|}{2v}(c-1),$$

and the dimensionless elastic constants, $\epsilon_c, \epsilon_y, \kappa_0, \mu_0$ and $k_{10} = \kappa_0 + 2\mu_0(1-1/d)$:

$$\frac{|\tilde{u}_1|^2}{4\gamma_1\chi_{n1}v}\epsilon_c = \epsilon_\phi, \quad (17)$$

$$\frac{|\tilde{u}_1|^2}{4v}\epsilon_y = \epsilon_\psi,$$

$$\frac{|\tilde{u}_1|^3}{8v^2}\kappa_0 = \kappa'_0,$$

$$\frac{|\tilde{u}_1|^3}{8v^2}\mu_0 = \mu'_0.$$

With these transformations, the free energy density becomes

$$\tilde{f}(c, y, \mu) = A_0 \left\{ y^2(1-y^2)^2 + \alpha(c+y^2-1)^2 \right\} + B_0$$

$$+ A_0 \left\{ [\epsilon_c(c-c_0) + \epsilon_y y^2] \nabla \cdot \mathbf{u} \right.$$

$$\left. + \frac{1}{2k_{10}} [\epsilon_c(c-c_0) + \epsilon_y y^2]^2 + f_{el}(\mu) \right\}, \quad (18)$$

where $A_0 = \frac{|\tilde{u}_1|^3}{8v^2}$ is a multiplicative constant with dimensions of energy, $B_0 = \frac{(\epsilon_\phi\phi_0)^2}{2k_{10}} - \frac{\chi_{n1}\Delta_0^2}{2}$ is an irrelevant additive constant, $\alpha = \frac{\gamma_1^2\chi_{n1}}{|\tilde{u}_1|}$ is a positive dimensionless constant that measures the coupling between c and y , and f_{el} is the dimensionless elastic energy:

$$f_{el}(\mu) = \frac{1}{2}\kappa_0(\nabla \cdot \mathbf{u})^2 + \mu_0 \sum_{i,j} \left(\mu_{ij} - \frac{\delta_{ij}}{d} \nabla \cdot \mathbf{u} \right)^2. \quad (19)$$

Dropping the additive constant B_0 and scaling the free energy by A_0 , we define the dimensionless energy $f(c, y, \mu)$ as

$$f(c, y, \mu) = f_1(c, y) + f_2(c, y, \mu),$$

$$f_1(c, y) = y^2(1-y^2)^2 + \alpha(c+y^2-1)^2, \quad (20)$$

$$f_2(c, y, \mu) = \frac{1}{2k_{10}} [\epsilon_c(c-c_0) + \epsilon_y y^2]^2$$

$$+ [\epsilon_c(c-c_0) + \epsilon_y y^2] \nabla \cdot \mathbf{u} + f_{el}(\mu).$$

$f_1(c, y)$ corresponds to a free energy with three coexisting minima and without coupled elastic fields [10]. Minimizing this energy with respect to c , at fixed y , gives $c = 1 - y^2$. In the (c, y) plane, the disordered minimum is at $(1, 0)$, while the degenerate ordered minima are at $(0, \pm 1)$. Under the assumption of constant elastic moduli that we have used so far, and in absence of external strain, the elastic field satisfies

$$\nabla \cdot \mathbf{u} = -\frac{1}{k_{10}} [\epsilon_c(c-c_0) + \epsilon_y y^2],$$

$$\frac{\partial u_i}{\partial x_j} = -\frac{\epsilon_c}{k_{10}} \frac{\partial^2 W_c}{\partial x_j \partial x_i} - \frac{\epsilon_y}{k_{10}} \frac{\partial^2 W_y}{\partial x_j \partial x_i}, \quad (21)$$

$$\nabla^2 W_c = c - c_0,$$

$$\nabla^2 W_y = y^2.$$

If we replace these expressions in $f_2(c, y, \mu)$, we find that it vanishes identically [13], since the elastic effects have been eliminated through the process of rescaling.

B. Concentration and order parameter dependent elastic moduli

We will generalize the energy so that the elastic coefficients depend on both c and y . We will also deal with a more general case and include an anisotropic cubic term and external strains. We will define generalized elastic moduli M, K , and B such that for an isotropic system,

these moduli are given by

$$\begin{aligned} M &= \mu, \\ K &= \kappa = \lambda + \frac{2}{d}\mu, \\ B &= 0. \end{aligned} \quad (22)$$

Here κ and μ are the bulk and shear elastic moduli [11] in their dimensionless form. For the cubic system, the generalized elastic moduli become

$$\begin{aligned} M &= C_{44}, \\ K &= C_{12} + \frac{2}{d}C_{44}, \\ B &= C_{11} - C_{12} - 2C_{44}. \end{aligned} \quad (23)$$

Here the C_{ij} 's are the stiffness coefficients, and the anisotropy is defined as $\xi = B/C_{44}$.

The simplest functional form we can write for the elastic moduli is

$$\begin{aligned} K &= k_0 + k_c(c - c_0) + k_y y^2, \\ M &= m_0 + m_c(c - c_0) + m_y y^2, \\ B &= b_0 + b_c(c - c_0) + b_y y^2. \end{aligned} \quad (24)$$

If we set all the coefficients to zero, except for m_0 and k_0 , we recover the energy density analyzed previously. The moduli take different values in phases with different concentrations. This concentration and order parameter dependence turns out to be a key factor determining the morphology of domains. The free energy density $f(c, y, \mu)$ is given by Eq. (21) with the elastic free energy density expressed in terms of the generalized elastic moduli:

$$\begin{aligned} f_{el}(\mu) &= \frac{1}{2}K(\nabla \cdot \mathbf{u})^2 + M \sum_{i,j} \left(\mu_{ij} - \frac{\delta_{ij}}{d} \nabla \cdot \mathbf{u} \right)^2 \\ &\quad + \frac{1}{2}B \sum_i u_{ii}^2. \end{aligned} \quad (25)$$

The elastic strain tensor is

$$\begin{aligned} \sigma_{ij} &= [\epsilon_c(c - c_0) + \epsilon_y y^2 + K \nabla \cdot \mathbf{u} + B u_{ii}] \delta_{ij} \\ &\quad + 2M \left(\mu_{ij} - \frac{\delta_{ij}}{d} \nabla \cdot \mathbf{u} \right). \end{aligned} \quad (26)$$

We want to express the elastic field in terms of the concentration and order parameter, so that the last two terms in $f_2(c, y, \mu)$, Eq. (21), get replaced by an effective energy that describes the interactions between the fluctuations of the concentration and order parameter [7]. This free energy will be computed to first order in the elastic coefficients k_α , m_α , and b_α , where $\alpha = y$ or $\alpha = c$. We call Δ_{el}^α the part of the functional derivative of the energy due to the elastic field, i.e.,

$$\begin{aligned} \Delta_{el}^\alpha &= (2y)^\alpha \left[\frac{1}{2} k_\alpha (\nabla \cdot \mathbf{u})^2 + \epsilon_\alpha \nabla \cdot \mathbf{u} \right. \\ &\quad \left. + \frac{m_\alpha}{4} \sum_{i,j} \left(\frac{\partial u_i}{\partial x_j} + \frac{\partial u_j}{\partial x_i} - \frac{2}{d} \delta_{ij} \nabla \cdot \mathbf{u} \right)^2 \right. \\ &\quad \left. + \frac{1}{2} b_\alpha \sum_i u_{ii}^2 \right], \end{aligned} \quad (27)$$

where $(2y)^y = 2y$ and $(2y)^c = 1$. We see that, except for the second term, Δ_{el}^α is already first order in the elastic moduli, so we need to compute $\frac{\partial u_i}{\partial x_j}$ only to zeroth order, and then we need a correction to first order for the term $\epsilon_\alpha \nabla \cdot \mathbf{u}$. For simplicity we will assume that c and y are homogeneous within the boundaries of the region of interest, such that $\delta c = \delta y = 0$ along the boundary. We will also assume an external stress at the boundary, producing an affine deformation $\langle \frac{\partial u_i}{\partial x_j} \rangle = A_{ij}$.

To start, we apply the condition of equilibrium, Eq. (4), and only keep the terms to zeroth order. To this order of approximation we can write the trace of the strain tensor for the isotropic system as

$$\nabla \cdot \mathbf{u} = \text{Tr} A - \frac{[\epsilon_c(c - c_0) + \epsilon_y y^2]}{\lambda_0 + 2\mu_0}. \quad (28)$$

To solve for the cubic system, we go into Fourier space and with the definition

$$\chi(\hat{\mathbf{k}}) = \sum_i \frac{\hat{\mathbf{k}}_i^2}{C_{44}^0(1 + \xi \hat{\mathbf{k}}_i^2)} \quad (29)$$

we get

$$i\mathbf{k} \cdot \mathbf{u}_{\mathbf{k}} = - \frac{\chi(\hat{\mathbf{k}})[\epsilon_c c_{\mathbf{k}} + \epsilon_y (y^2)_{\mathbf{k}}]}{[1 + (C_{12}^0 + C_{44}^0)\chi(\hat{\mathbf{k}})]}, \quad (30)$$

where $(y^2)_{\mathbf{k}}$ is a shorthand notation, $(y^2)_{\mathbf{k}} = \int d\mathbf{q} y_{\mathbf{k}} y_{\mathbf{k}-\mathbf{q}}$. A linear approximation in the anisotropy gives

$$\begin{aligned} \nabla \cdot \mathbf{u} &= \text{Tr} A - \frac{[\epsilon_c(c - c_0) + \epsilon_y y^2]}{(C_{12}^0 + 2C_{44}^0)} \\ &\quad + \frac{\xi C_{44}^0 [\epsilon_c(c - c_0) + \epsilon_y y^2]}{(C_{12}^0 + 2C_{44}^0)^2} \\ &\quad - \frac{\xi C_{44}^0}{(C_{12}^0 + 2C_{44}^0)^2} \frac{1}{\nabla^2} \\ &\quad \times \sum_{i \neq j} \nabla_i^2 \nabla_j^2 \frac{1}{\nabla^2} [\epsilon_c(c - c_0) + \epsilon_y y^2]. \end{aligned} \quad (31)$$

To zeroth order, the strain tensor is

$$\frac{\partial u_i}{\partial x_j} = A_{ij} - \frac{\epsilon_c}{k_{10}} \frac{\partial^2 W_c}{\partial x_j \partial x_i} - \frac{\epsilon_y}{k_{10}} \frac{\partial^2 W_y}{\partial x_j \partial x_i}, \quad (32)$$

where $k_{10} = \lambda_0 + 2\mu_0$ for the isotropic system, and $k_{10} = C_{12}^0 + 2C_{44}^0$ for the cubic system.

We can define a traceless external strain tensor [7]

$$S_{ij} = A_{ij} + A_{ji} - \frac{2}{d} \delta_{ij} \text{Tr} A \quad (33)$$

and with it, we construct the tensor V_{ij} , which is first order in the elastic moduli:

$$V_{ij}^\alpha = m_\alpha S_{ij} + \frac{b_\alpha}{2} S_{ii} \delta_{ij}. \quad (34)$$

Now we introduce Eq. (32) back into Eq. (7) and compute the corrections to first order in $\nabla \cdot \mathbf{u}$. In doing so, we neglect the corrections to k_{10} originating from the coefficients k_α . We also neglect the terms that renormalize the

coefficients ϵ_α , [$\epsilon_\alpha \rightarrow \epsilon_\alpha + (k_\alpha + b_\alpha/d)\text{Tr}A$], since these corrections vanish in absence of external strain, and in most cases are negligible. After some algebra, we get an expression made up of eight terms:

$$\begin{aligned} \frac{\Delta_{el}^\alpha}{(2y)^\alpha} = & \Delta_0^\alpha - \frac{\epsilon_\alpha}{k_{10}} [\epsilon_c(c - c_0) + \epsilon_y y^2] - \frac{1}{k_{10}} \left[\sum_{i,j} (\epsilon_\alpha V_{ij}^c + \epsilon_c V_{ij}^\alpha) \frac{\partial^2 W_c}{\partial x_i \partial x_j} + \sum_{i,j} (\epsilon_\alpha V_{ij}^y + \epsilon_y V_{ij}^\alpha) \frac{\partial^2 W_y}{\partial x_i \partial x_j} \right] \\ & + \frac{m_\alpha}{k_{10}^2} \left[\epsilon_c \left(\frac{\partial^2 W_c}{\partial x_j \partial x_i} - \frac{\delta_{ij}}{d} (c - c_0) \right) + \epsilon_y \left(\frac{\partial^2 W_y}{\partial x_j \partial x_i} - \frac{\delta_{ij}}{d} y^2 \right) \right]^2 \\ & + \frac{2\epsilon_\alpha}{k_{10}^2} \frac{1}{\nabla^2} \sum_{i,j} \frac{\partial^2}{\partial x_i \partial x_j} \left[(m_c(c - c_0) + m_y y^2) \left(\epsilon_c \frac{\partial^2 W_c}{\partial x_j \partial x_i} - \frac{\delta_{ij}}{d} \epsilon_c (c - c_0) + \epsilon_y \frac{\partial^2 W_y}{\partial x_j \partial x_i} - \frac{\delta_{ij}}{d} \epsilon_y y^2 \right) \right] \\ & - \frac{b_0 \epsilon_\alpha}{k_{10}^2} \left[\epsilon_c \left(\frac{1}{\nabla^2} \sum_{i \neq j} \nabla_i^2 \nabla_j^2 W_c - (c - c_0) \right) + \epsilon_y \left(\frac{1}{\nabla^2} \sum_{i \neq j} \nabla_i^2 \nabla_j^2 W_y - y^2 \right) \right] \\ & + \frac{b_\alpha}{2k_{10}^2} \sum_i \left(\epsilon_c \frac{\partial^2 W_c}{\partial x_i^2} + \epsilon_y \frac{\partial^2 W_y}{\partial x_i^2} \right)^2 + \frac{\epsilon_\alpha}{k_{10}^2} \frac{1}{\nabla^2} \sum_i \frac{\partial^2}{\partial x_i^2} \left[(b_c(c - c_0) + b_y y^2) \left(\epsilon_c \frac{\partial^2 W_c}{\partial x_i^2} + \epsilon_y \frac{\partial^2 W_y}{\partial x_i^2} \right) \right]. \end{aligned} \quad (35)$$

The constant Δ_0^α is a function of the external strain, and is zero when the external stress is zero. The integration of Δ_{el}^α with respect to the order parameter and to the concentration gives rise to different interactions.

1. Effective local interaction

The first two terms of Eq. (35) represent the contribution of the constant isotropic elastic moduli. Integrating, we get

$$f'_{eff} = \Delta_0^c (c - c_0) + \Delta_0^y y^2 - \frac{1}{2k_{10}} [\epsilon_c (c - c_0) + \epsilon_y y^2]^2. \quad (36)$$

If we introduce this expression back in Eq. (21), we see that we are left with an effective local interaction energy of the form

$$f_{eff} = \Delta_0^c (c - c_0) + \Delta_0^y y^2 + y^2 (1 - y^2)^2 + \alpha (c + y^2 - 1)^2. \quad (37)$$

In absence of external stress $\Delta_0^\alpha = 0$, and we are left with the effective energy found in the preceding section. The effective local interaction absorbs all the contributions that come from the constant isotropic elastic moduli. All the remaining contributions in the effective energy originate either from the varying part of the elastic moduli or from the anisotropy, and they are long range.

2. Long-range dipolar interaction

Since the correction due to b_α in V_{ij}^α is very small, we neglect it. The third term in Eq. (35) gives the Δ_{el}^α due to the external stress. In general, it produces an anisotropic deformation. The integration of these terms gives

$$f_d = \frac{1}{k_{10}} \sum_{i,j} S_{ij} \left(\epsilon_c \frac{\partial c}{\partial x_i} + \epsilon_y \frac{\partial y^2}{\partial x_i} \right) \frac{1}{\nabla^2} \left(m_c \frac{\partial c}{\partial x_j} + m_y \frac{\partial y^2}{\partial x_j} \right). \quad (38)$$

A precipitate under the field produced by the exter-

nal strain tends to deform in particular directions given by the relation among the components of the tensor \mathbf{S} . This tensor also determines the form of the interaction between different precipitates; for instance, for two ellipsoidal precipitates A and B , of d -dimensional volumes V_A, V_B , a distance r_{AB} apart, this interaction is proportional to $V_A V_B \frac{(\hat{r}_{AB} \cdot \mathbf{S} \cdot \hat{r}_{AB})}{r_{AB}^d}$.

3. Long-range Eshelby interaction

The fourth and fifth terms in Eq. (35) give rise to a long-range interaction due to the difference of shear moduli in the ordered and disordered phases. The integration of these two terms gives

$$\begin{aligned} f_E = & \frac{1}{k_{10}^2} [m_c (c - c_0) + m_y y^2] \\ & \times \sum_{i,j} \left[\epsilon_y \left(\frac{\partial^2 W_y}{\partial x_j \partial x_i} - \frac{\delta_{ij}}{d} y^2 \right) \right. \\ & \left. + \epsilon_c \left(\frac{\partial^2 W_c}{\partial x_j \partial x_i} - \frac{\delta_{ij}}{d} (c - c_0) \right) \right]^2. \end{aligned} \quad (39)$$

Eshelby was the first to calculate a pairwise interaction between spherical precipitates where the elastic moduli are different [2]. This interaction is valid as long as the precipitates remain spherical. Onuki and Nishimori have shown the relevance of shape deformations from sphericity in the presence of elastic misfits: the harder domains deform from sphericity to cancel elastic fields produced by other harder domains and to become elastically isotropic, while the softer regions are elastically anisotropic (uniaxially deformed). They have also found that the domain growth is dramatically slowed down in the presence of this interaction, when the elastic field is coupled to a concentration with model B dynamics. For volume fractions of the soft phase of 50% or less, they have found that the modulus inhomogeneity drives the system into metastable glassy states after the asymmetric elastic deformations.

4. Long-range cubic interaction

The symmetry properties of the surface energy in cubic crystals are, for small gradients, isotropic and proportional to the square of the gradient terms in the energy. All the anisotropies in the early stages of spinodal decomposition come exclusively from the elastic anisotropy [9]. The last three terms of Eq. (35) arise due to the cubic anisotropy. The sixth term in b_0 creates an effective energy of the form

$$f_{cub} = -\frac{\xi C_{44}^0}{2(C_{12}^0 + 2C_{44}^0)^2} \left[\sum_{i \neq j} [\nabla_i \nabla_j (\epsilon_c W_c + \epsilon_y W_y)]^2 - [\epsilon_c (c - c_0) + \epsilon_y y^2]^2 \right]. \quad (40)$$

After a quench, spinodal decomposition is triggered by fluctuations in the concentration and order parameter along the softest directions. The domains start to grow on the habit planes, which are perpendicular to the softest directions. It can be shown that for $\xi < 0$, the fluctuations first become unstable along the $\langle 100 \rangle$ directions for $d = 3$ ($\langle 10 \rangle$ for $d = 2$); while for $\xi > 0$, they first become unstable along the $\langle 111 \rangle$ directions for $d = 3$ ($\langle 11 \rangle$ for $d = 2$). In the presence of external stresses, a competition arises between the inherent cubic anisotropy and the external anisotropy due to the applied stress.

The last two terms with b_α contribute a correction to f_{cub} :

$$f_{cub}^{(1)} = \frac{1}{2(C_{12}^0 + 2C_{44}^0)^2} [b_c (c - c_0) + b_y y^2] \times \sum_i \left(\epsilon_y \frac{\partial^2 W_y}{\partial x_i^2} + \epsilon_c \frac{\partial^2 W_c}{\partial x_i^2} \right). \quad (41)$$

In cases where the anisotropy $\xi = (C_{11}^0 - C_{12}^0 - 2C_{44}^0)/C_{44}^0$ is a small quantity, the corrections to it are still smaller, so one could neglect $f_{cub}^{(1)}$.

C. Langevin equations

For our numerical study, we only consider effective local interactions (that simply renormalize the free energy) and long-range Eshelby interactions; i.e., we assume no external stress and no anisotropy in the system (and we set to zero both the anisotropy ξ and the external strain \mathbf{S}). The study of the long-range Eshelby interaction is particularly interesting for the model C system, since this system allows us to choose either the disordered phase or the ordered phase to be the hard phase, a feature that is not present in model B. We now introduce the corresponding dynamical equations assuming that the dynamical processes related to the elastic displacement are much faster than the processes related to the changes in the concentration and order parameter. We use the adiabatic approximation for the elastic field such that for a given concentration and order parameter field at time t , the displacement vector $\mathbf{u}(\mathbf{r})$ is such that it minimizes the total free energy. The evolution of the concentration

and order parameter is then described by the Langevin equations:

$$\frac{\partial y}{\partial t} = -\Gamma_y \left[\frac{\partial f(c, y, \mu)}{\partial y} - l_y^2 \nabla^2 y \right] + \xi_y, \quad (42)$$

$$\frac{\partial c}{\partial t} = \Gamma_c \nabla^2 \left[\frac{\partial f(c, y, \mu)}{\partial c} - l_c^2 \nabla^2 c \right] + \xi_c, \quad (43)$$

where $f(c, y, \mu)$ is the dimensionless energy obtained in the preceding section, consisting of two terms: $f(c, y, \mu) = f_{eff} + f_E$. As a first approach, we neglect all other hydrodynamical modes. The new mobilities and the new coefficients of the square gradients are given in terms of the original mobilities Γ_ψ and Γ_ϕ and the original coefficients l_ψ^2 and l_ϕ^2 :

$$\begin{aligned} \Gamma_y &= \frac{|\bar{u}_1|^2}{4v} \Gamma_\psi, \\ \Gamma_c &= \frac{|\bar{u}_1|}{2(\gamma_1 \chi_{n1})^2} \Gamma_\phi, \\ l_y^2 &= \frac{4v}{|\bar{u}_1|^2} l_\psi^2, \\ l_c^2 &= \frac{2(\gamma_1 \chi_{n1})^2}{|\bar{u}_1|} l_\phi^2. \end{aligned} \quad (44)$$

Here ξ_c and ξ_y are stochastic variables verifying the fluctuation-dissipation relation:

$$\langle \xi_y(\mathbf{r}, t) \xi_y(\mathbf{r}', t') \rangle = 2\tau \Gamma_y \delta(\mathbf{r} - \mathbf{r}') \delta(t - t'), \quad (45)$$

$$\langle \xi_c(\mathbf{r}, t) \xi_c(\mathbf{r}', t') \rangle = -2\tau \Gamma_c \nabla^2 \delta(\mathbf{r} - \mathbf{r}') \delta(t - t'),$$

where τ is the dimensionless thermal energy: $\tau = k_B T \frac{8v^2}{|\bar{u}_1|^8}$.

III. SIMULATIONS

A. Numerical integration

Using the notation $b_{ij} = \epsilon_y \left(\frac{\partial^2 W_y}{\partial x_j \partial x_i} - \frac{\delta_{ij}}{d} y^2 \right) + \epsilon_c \left(\frac{\partial^2 W_c}{\partial x_j \partial x_i} - \frac{\delta_{ij}}{d} (c - c_0) \right)$ and $Q = \sum_{i,j} b_{ij}^2$, the previous Langevin equations become

$$\begin{aligned} \frac{\partial y}{\partial t} &= -\Gamma_y \left[\frac{\partial f_{eff}(c, y)}{\partial y} - l_y^2 \nabla^2 y + 2y m_y Q \right. \\ &\quad \left. + 4y \epsilon_y \frac{1}{\nabla^2} \sum_{i,j} \frac{\partial^2}{\partial x_j \partial x_i} x_i \{ m_c (c - c_0) \right. \\ &\quad \left. + m_y y^2 \} b_{ij} \right], \end{aligned} \quad (46)$$

$$\begin{aligned} \frac{\partial c}{\partial t} &= \Gamma_c \nabla^2 \left(\frac{\partial f_{eff}(c, y)}{\partial c} - l_c^2 \nabla^2 c + m_c Q \right) \\ &\quad + 2\epsilon_c \sum_{i,j} \frac{\partial^2}{\partial x_j \partial x_i} \{ m_c (c - c_0) \\ &\quad + m_y y^2 \} b_{ij}. \end{aligned} \quad (47)$$

TABLE I. Parameters used in the simulation.

Run	c_0	ϵ_y	ϵ_c	m_y	m_c
A	1/3	1	0	0.22	0.0
B	2/3	1	0	0.22	0.0
C	1/3	0	1	0.0	0.22
D	2/3	0	1	0.0	0.33

In these equations the coefficients ϵ_α are redefined so that $\epsilon_\alpha \equiv \frac{\epsilon_\alpha}{k_l^\alpha}$, and we have neglected noise, whose importance we will discuss later.

To solve for the operator $\frac{1}{\nabla^2}$, we found that it was convenient and more precise to use pseudospectral methods. It was found necessary to use an “isotropic” form of the Laplacian (which couples nearest and next-nearest neighbor cells) and of its representation in Fourier space Δ_K : $\Delta_K = [\cos(k_x dx)\cos(k_y dy) + \cos(k_x dx) + \cos(k_y dy) - 3]/dx^2$, where we used $dx = dy$. Notice that in Fourier space, $W_c = -\frac{c_0}{k^2}$ and $W_y = -\frac{(y^2)_k}{k^2}$, with the notation $(y^2)_k = \int d\mathbf{q} y_{\mathbf{k}} y_{\mathbf{k}-\mathbf{q}}$.

We performed quenches from an initially disordered state to a state inside the classical spinodal. For these quenches, we used two values of the concentration: either $c_0 = 1/3$ or $c_0 = 2/3$ [14]. For all these quenches, we set $\Gamma_c, \Gamma_y, l_y^2$, and l_c^2 to unity and $\alpha = 4$. The Langevin equations were solved numerically using Euler’s Method on a two-dimensional grid with a finite difference scheme. Periodic boundary conditions were used throughout. The spatial and temporal mesh sizes were chosen to avoid possible spurious unphysical solutions resulting from the subharmonic bifurcation. The spatial mesh size was taken to be $\Delta x = 1.2$. The complicated form of the energy imposes constraints on the time mesh size, which was chosen as $\Delta t = 0.01$ or $\Delta t = 0.03$, according to the particular set of parameters. This simulation takes about 370 CPU hours in a Hewlett-Packard 700 for an average run with $\Delta t = 0.03$ up to $t = 10\,000$. Our initial distribution of y ’s was specified by a random uniform distribution in the range $(-0.1, 0.1)$, while the initial distribution of c ’s was specified by a similar random distribution in the range $(c_0 - 0.1, c_0 + 0.1)$.

Table I summarizes the elastic field parameters used. For each set of parameters, we carried out four runs on a 128x128 square grid and one run on a 256x256 square grid. For each set we computed the nonequilibrium pair correlation function for both the conserved variable c and the nonconserved order parameter y , as well as their corresponding circular averages. We also computed the typical length scale $R_c(t)$ associated with domains of c . This was defined as the smallest value of r for which $C_c(r, t) = 0$ at time t ; as well as $R_y(t)$, the typical length scale associated with domains of the variable y and defined as the value of r for which $C_y(r, t) = 1/2$ at time t .

B. Results

Here we present the results of our simulation. Figures 2(a) and 2(b) show the time evolution for a simple model C system for $c_0 = 1/3$ (or normalized con-

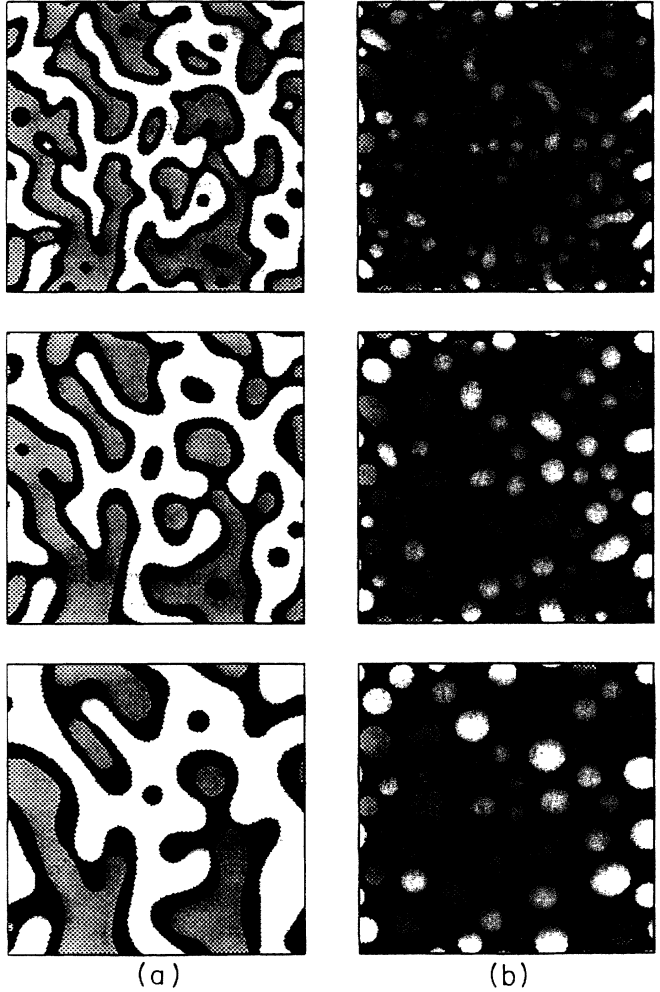


FIG. 2. Typical configurations for a model C system quenched into the order-disorder coexistence region, and with parameters chosen such that the disordered phase (black) forms a wetting layer that wraps the ordered domains with opposite sign (white or gray). The times shown in the picture correspond to $\tau = 150$, $\tau = 450$, and $\tau = 1500$, from top to bottom. (a) shows a quench with $c_0 = 1/3$ and (b) shows a quench with $c_0 = 2/3$.

centration $\chi = -1/3$) and $c_0 = 2/3$ ($\chi = +1/3$) [14]. The energy is asymmetric with respect to χ [10], so that $\chi = -1/3$ gives a convoluted morphology of percolating domains while $\chi = +1/3$ gives isolated circular clusters of ordered phase. For these configurations, there is a macroscopic wetting layer of disordered phase (indicated by black color) between two ordered phases of opposite sign (indicated by white and gray colors).

We want to see how these morphologies are altered when we couple an elastic field to the concentration or order parameter. Notice that the shear modulus for the ordered phase is $\mu_{ord} = -m_c c_0 + m_y$ while for the disordered phase it is $\mu_{dis} = m_c(1 - c_0)$ so that $\Delta\mu = \mu_{ord} - \mu_{dis} = m_y - m_c$. If $m_y > m_c$, then $\Delta\mu > 0$ and the ordered phase is the hard phase. Conversely, if $m_c > m_y$, $\Delta\mu < 0$ and the disordered phase is the hard phase. As stated in Table I, we will couple a field to the concentration ($\epsilon_c, m_c \neq 0, \epsilon_y = m_y = 0$) or to the order

parameter ($\epsilon_y, m_y \neq 0$, $\epsilon_c = m_c = 0$), for both $c_0 = 1/3$ and $c_0 = 2/3$.

Figures 3(a), 3(b), 4(a), and 4(b) show the resulting morphology for runs A, B, C, and D. In all these configurations, the hard phase always forms the precipitate (i.e., the individual domains) while the soft phase always forms the matrix (i.e., the percolating background). In runs A and B, $m_y = 0.22$ and $m_c = 0.0$, which means that the ordered phase forms the precipitate (whose domains alternate in sign). Thus, due to the elastic forces, the majority phase ordered domains in run A ($c_0 = 1/3$) form isolated clusters (wrapped by the minority phase) and no longer percolate through the system, as it happens in the model C system without elastic forces [Fig. 2(a)]. For run B ($c_0 = 2/3$), the elastic forces do not alter much the morphology from that of the model C system, where the ordered domains (which are minority phase for this concentration) already form isolated clusters.

In runs C and D [Figs. 4(a) and 4(b)], $m_c = 0.22$ and $m_c = 0.33$, respectively, while $m_y = 0.0$ for both. This means that the disordered phase forms the precipitate.

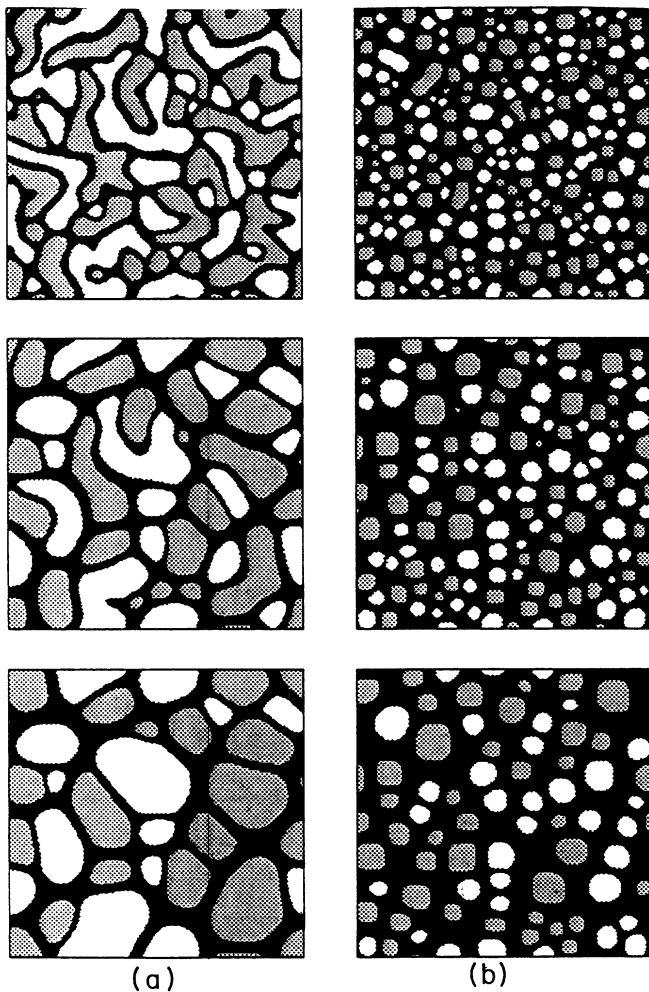


FIG. 3. Configurations where the ordered phase is the hard phase. (a) shows run A ($c_0 = 1/3$) and (b) shows run B ($c_0 = 2/3$). Times correspond to $\tau = 300, 1500$, and 6000 , from top to bottom.

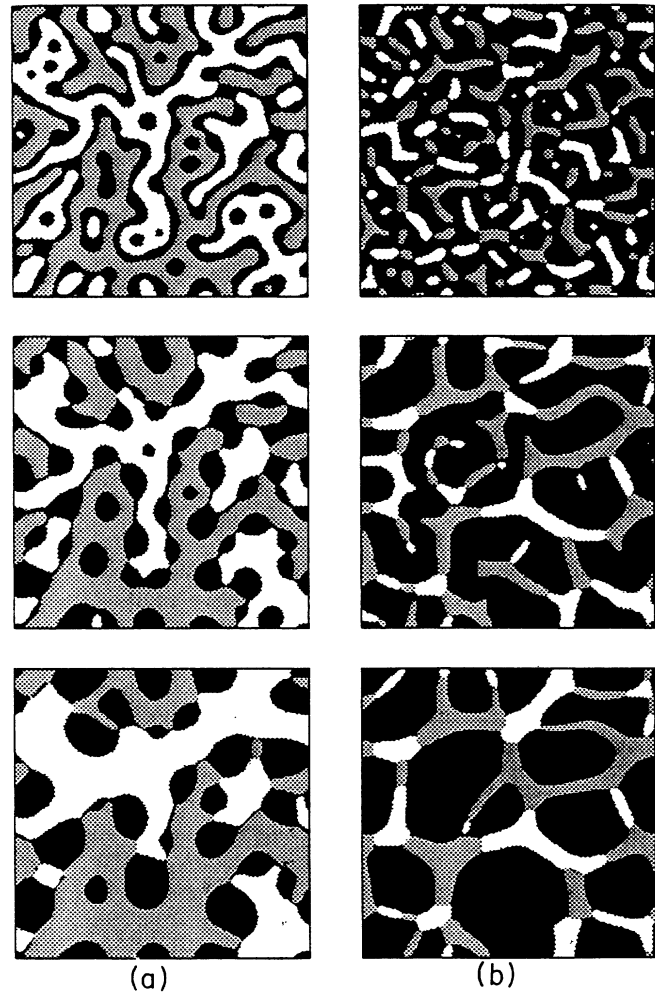


FIG. 4. Configurations where the disordered phase is the hard phase. (a) shows run C ($c_0 = 1/3$) and (b) shows run D ($c_0 = 2/3$). Times correspond to $\tau = 300, 1500$, and 6000 , from top to bottom.

Interesting competing effects arise: on the one hand, due to the nature of the model C quench, the disordered phase tends to form the macroscopic wetting layer between the ordered phases; on the other, due to the presence of the elastic forces, the disordered phase tends to form isolated domains, such that part of the order-disorder interfaces [$(y = +1)-(y = 0)$ and $(y = -1)-(y = 0)$] disappears to form order-order interfaces [$(y = +1)-(y = -1)$]. Note that for run C at early times, surface forces dominate over elastic forces and a wetting layer is formed. But as time evolves and the domains become larger, elastic forces compete and thin this layer. This is graphic evidence that surface forces and elastic forces have different scaling behavior with respect to changes in the length scale. A similar competition arises in run D although, in this case, the elastic forces become dominant at much earlier times [compare the early-time pictures in Figs. 2(b) and 4(b)]. In run D, the length of the order-order interfaces is less than that in run C, so the wetting layer is absorbed faster.

These competing effects can also happen in the inverse regime. A quench in the “drying” regime of model C

produces isolated clusters of the disordered phase, which no longer wet the interface between the ordered phases. Such a quench shows both types of interface: order-disorder and order-order. The addition of an elastic interaction where the ordered phase is the hard phase will again bring competing effects; the elastic energy favors a configuration where the disordered soft phase percolates and wraps the hard domains.

The elastic forces slow down the growth of the domains. This effect manifests itself at late times when the domains are large. Thus the slowing down will occur sooner in runs A and D, where the majority phase forms the precipitate than in runs B and C, where the minority phase forms the precipitate. Particularly, for some runs, the domains of the ordered phase may become very large (see, for example, run C). In this case, our results for $R_y(t)$ lack some self-averaging and could be affected by finite-size effects [qualitatively the behavior of $R_y(t)$ is similar to that of $R_c(t)$]. On the other hand, $R_c(t)$ presents much better self-averaging and smaller size effects, although runs A and D are more vulnerable to finite-size effects than runs B and C. To study these effects, we chose run A and did two runs on a system of $N = 256$, eight runs for $N = 128$, and 32 runs for $N = 64$. Within error bars, we found agreement in the curves of $R_c(t)$ and $R_y(t)$.

Figure 5 shows the time evolution of $R_c(t)$. In general, the effective growth exponent n decreases with time. For instance, for late times $n = 0.14$ for run A. We believe that these effective exponents correspond to a transient stage and we expect the domain growth to stop for very late times. This expectation contrasts with our result for run C, where we measure an effective exponent $n = 0.29$ for the latest time ($\tau = 12\,000$). This could be due to the following. (i) *Lack of statistics*. A growth exponent obtained with a single run must be considered only indicative. (ii) *Small amount of hard phase*. In a study with model B with elastic forces, Onuki and Nishimori [7] showed that the effect of elastic forces in domain growth depends on concentration. In particular, they found that domain growth was dramatically slowed down (and it tended to stop) for concentrations of the

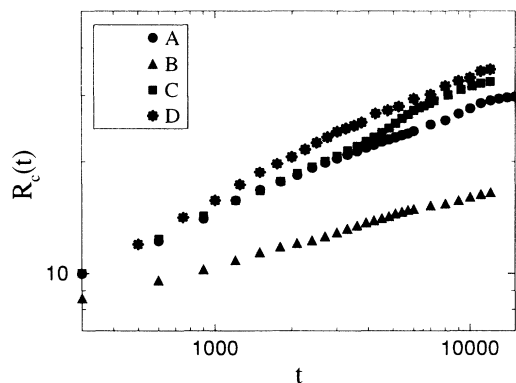


FIG. 5. Time dependence of the characteristic domain length $R_c(t)$ (as computed from the correlation function) for the different runs.

hard phase higher than 0.5. For lower concentrations they did not see the domains stop. For runs C and B, the volume fraction of the hard phase is less than 0.5. (iii) *Reduction of the wetting layer*. In spite of a possible lack of statistics, this run presents some peculiarities absent in the rest of the runs. It is the only case in which the morphology of the hard domains is changing in time, due to the competition between surface and elastic forces. This could affect growth: the concentration is leaving the original wetting layer to join the spherical domains. Yet, all these domains are still connected through threads of this wetting layer. In this case diffusion parallel to the wetting layer could be very important. Once the wetting layer has completely disappeared, the dominant mechanism is diffusion perpendicular to the interface of the domain; however, for the latest time of our simulation a thin wetting layer is still present.

In spite of our inconclusive results for run C, we believe that growth will finally stop and the system go into a glassy state, due to both the presence of conservation law and the elastic forces. In order to clarify this possibility we have followed two different approaches, (i) we have plotted the part of the functional derivative of the energy solely due to the elastic field, and (ii) we have studied the interface equations of motion, in order to separate the contributions from diffusion and from elastic forces.

Figure 6 shows the functional derivative of the elastic energy with respect to the concentration for the runs shown before. [For runs A and B, the elastic energy does not explicitly depend on $c(\mathbf{r})$. Assuming that near equilibrium $c = 1 - y^2$, we obtained the derivative with respect to c from the derivative with respect to y .] The white color corresponds to high positive derivative, the black color corresponds to negative derivative, and the

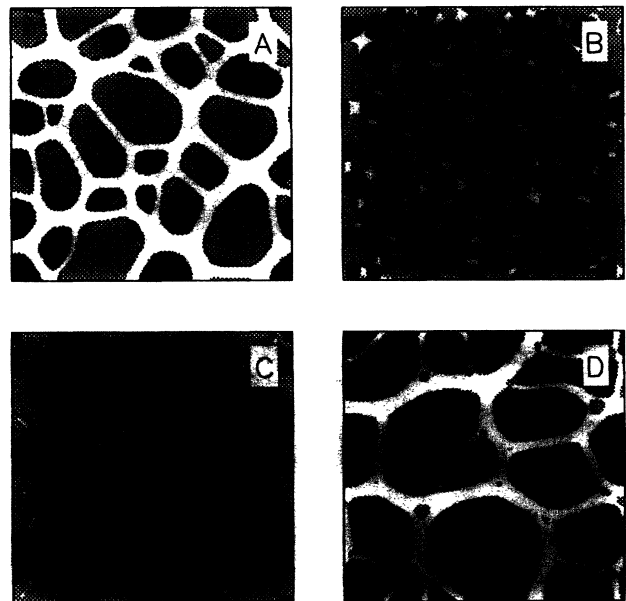


FIG. 6. Functional derivative of the elastic energy with respect to the concentration, $g = \delta F_{el} / \delta c$. The figures correspond to $\tau = 6000$, i.e., the last configurations shown in Figs. 3 and 4. The color scale is the following: white, $g > 0.2$; gray, $0 \leq g \leq 0.2$; black, $g < 0$.

gray color to intermediate positive values. The gray and white regions repel particles belonging to the black regions, so that it will cost energy if a particle in a black domain is to move to another black domain. The only way a domain can grow is by diffusion of particles, due to the conservation law associated with the concentration. But this diffusion process will be hindered by these elastic barriers. The existence of the barriers is always expected: the inhomogeneity of the system creates elastic misfits which translate into large deformations at the boundary of a hard phase precipitate. A hard phase deformation is energetically more expensive than a soft phase deformation, so these deformations occur in the soft phase immediately surrounding the hard phase precipitate. The surface energy of the domains decays like $1/R$, but the elastic energy does not, as dimensional analysis shows. At very early times the domain growth is dominated by the surface energy, but at very late times the elastic energy takes over. There is a crossover radius R_E , which is roughly given by $R_E \sim \sigma_{10} |(m_y - m_c) [\epsilon_y y^2 + \epsilon_c (c - c_0)]|^{-1}$, where y^2 and c take their corresponding saturation value inside the domains. For $R \gg R_E$ the elastic energy becomes dominant and leads to a metastable glassy state.

In the Appendix we derive the interface equation of motion for the concentration following the method of Kawasaki and Ohta [15] [Eq. (A30)]:

$$\int G(\mathbf{r}(a), \mathbf{r}(a')) v(a') da' = \sigma(d-1) \left[\frac{1}{R_c} - \frac{1}{r(a)} \right] - (\Delta\epsilon)^2 |\Delta\mu| I_D(\mathbf{r}(a)). \quad (48)$$

Here a is the $(d-1)$ -dimensional coordinate along the interface of a domain; $G(\mathbf{r}(a), \mathbf{r}(a'))$ is the Green's function evaluated at two points a and a' not necessarily belonging to the same domain; $v(a')$ is the velocity normal to the surface; σ is the order-disorder surface tension; R_c is the mean critical domain length; $\frac{1}{r(a)}$ is the mean curvature of the surface; $\Delta\epsilon = \epsilon_y - \epsilon_c$; $\Delta\mu = \mu_y - \mu_c$; D is the region comprised by the precipitate domains, and $I_D(\mathbf{r}(a))$ is given by

$$I_D(\mathbf{r}(a)) = \sum_{ij} \int_D d\mathbf{r}' \int_D d\mathbf{r}'' \left[2M_{ij}(\mathbf{r}(a), \mathbf{r}') M_{ij}(\mathbf{r}', \mathbf{r}'') + M_{ij}(\mathbf{r}(a), \mathbf{r}') M_{ij}(\mathbf{r}(a), \mathbf{r}'') \right], \quad (49)$$

with

$$M_{ij}(\mathbf{r}, \mathbf{r}') = \frac{\partial^2 G(\mathbf{r}, \mathbf{r}')}{\partial x_j \partial x_i} - \frac{\delta_{ij}}{d} \delta(\mathbf{r} - \mathbf{r}'). \quad (50)$$

In Eq. (48), $\Delta(\mathbf{r}(a)) = \sigma(d-1)/r(a) + (\Delta\epsilon)^2 |\Delta\mu| I_D(\mathbf{r}(a))$ is the chemical potential at $\mathbf{r}(a)$; the second term is the contribution from elasticity. Thus Eq. (48) simply means that domains with small chemical potential at the surface grow at the expense of those with higher chemical potential at the surface.

We show in the Appendix that the predictions given by these equations for a model B system consisting of a small volume fraction of hard phase spherical precipitates are contrary to our corresponding simulations. It

could be argued that the discrepancies between the theoretical predictions and the simulations are due to the assumption of spherical shapes, since the interaction among domains induces distortions from the spherical shape [7]. However, this effect is negligible in the limit of dilute systems and cannot be strong enough to dominate the other terms in the equation. We argue that these discrepancies are due to the existence of the elastic energy barriers, which are not considered in the theoretical formulation. The equations compare the chemical potential at the surface of two domains and neglect the important fact that when a particle goes from one domain to the other, it must necessarily pass through a region with even higher chemical potential.

In our opinion, Eq. (48) should be evaluated not at the interface but at a surface where the chemical potential is maximum. The new equation should read

$$\int G(\mathbf{z}(a), \mathbf{r}(a')) v(a') da' = h(t) - \Delta_{diff}(\mathbf{z}(a)) - (\Delta\epsilon)^2 |\Delta\mu| I_D(\mathbf{z}(a)), \quad (51)$$

where $\mathbf{z}(a)$ defines the new surface, $h(t)$ accounts for global conservation of particles, $\Delta_{diff}(\mathbf{z}(a))$ is the diffusive chemical potential in absence of elastic energy, and the last term is the elastic contribution.

We expect that the addition of noise to the simulation would allow the system to reach its absolute minimum, but the time the system will take to reach this minimum will increase exponentially with the height of the elastic barrier, so that the growth would be logarithmically slow for very long times.

IV. CONCLUSIONS

In this paper we have studied the effect of an elastic field in an order-disorder phase transition described by the dynamics corresponding to a model C system. The elastic field was coupled to both the concentration and the order parameter. By assuming that the elastic field relaxes very fast, and using the condition of mechanical equilibrium, we expressed it in terms of the conserved variable and the order parameter. We concentrated our study on the long-range Eshelby interaction that arises due to the difference of shear moduli in the ordered and disordered phases. We showed how this elastic interaction modifies dramatically the spinodal decomposition. By choosing the coefficients of the concentration and order parameter in the shear modulus, we were able to select the phase that forms the hard precipitate. Changes in morphology are more dramatic when there are competing effects between the wetting regime of the model C and the elastic energy. Thus, in the regime where the disordered phase wets the interface between the ordered domains, ordered phase precipitates form individual clusters but still keep this wetting property. However, disordered phase precipitates tend to form isolated relatively

spherical domains that no longer wet the order-order interface. Conversely, in the drying regime, the disordered phase tends to form isolated nonwetting clusters in absence of elastic fields but if it becomes the soft phase due to the presence of elastic strains, then it tends to percolate and wrap the hard ordered precipitates. The elastic field produced by elastic misfits alters not only the resulting morphology but also leads the system to very sluggish growth and to an eventual frozen metastable state.

ACKNOWLEDGMENTS

R.C.D. and C.S. acknowledge support by the NSERC of Canada. A.M.S. acknowledges support from Grant No. PB91-0090 of DGCyT (Spain). We would also like to thank Chuck Yeung for useful discussions.

APPENDIX

The important features of the late-stage dynamics are described by the motion of the interfaces. Here we first derive the interface equations of motion following the method of Kawasaki and Ohta [15] for a model B system. We show how the equations obtained for this system do not give the correct physics and we suggest how to modify them. Later we generalize this treatment for a model C system.

We start with the Eshelby interaction written for a model B system:

$$f_E = -g_c c \sum_{i,j} \left[\left(\frac{\partial^2 W}{\partial x_j \partial x_i} - \frac{\delta_{ij}}{d} \nabla^2 W \right) \right]^2, \quad (\text{A1})$$

with

$$\nabla^2 W = c$$

and $g_c = \epsilon_c^2 m_c > 0$. This choice of g_c simply states that if $c < 0$ the energy will be minimized by setting the shear strain to zero, while if $c > 0$ the energy will be minimized by maximizing the shear strain. In other words, the hard phase precipitate occurs for $c < 0$ and the soft phase background has $c > 0$.

We introduce the Green function $G(\mathbf{r}, \mathbf{r}')$:

$$\nabla^2 G(\mathbf{r}, \mathbf{r}') = \delta(\mathbf{r} - \mathbf{r}') \quad (\text{A2})$$

and the tensor M_{ij} :

$$M_{ij}(\mathbf{r}, \mathbf{r}') = \frac{\partial^2 G(\mathbf{r}, \mathbf{r}')}{\partial x_j \partial x_i} - \frac{\delta_{ij}}{d} \delta(\mathbf{r} - \mathbf{r}'). \quad (\text{A3})$$

The tensor M_{ij} is translational invariant over all the space Ω and verifies $\sum_i M_{ii} = 0$. With this definition, we can write

$$\begin{aligned} F[c] &= \int d\mathbf{r} \left[f(c) + \frac{1}{2} (\nabla c)^2 \right] \\ &\quad - g_c \sum_{i,j} \int d\mathbf{r} d\mathbf{r}' d\mathbf{r}'' M_{ij}(\mathbf{r}, \mathbf{r}') M_{ij}(\mathbf{r}', \mathbf{r}'') \\ &\quad \times c(\mathbf{r}) c(\mathbf{r}') c(\mathbf{r}''). \end{aligned} \quad (\text{A4})$$

For the interface description we use a curvilinear coordinate system such that u is the coordinate normal to the interface, $u = 0$ on the interface, and a is the $(d-1)$ -dimensional coordinate along the interface. We define the normal to the interface as $\hat{\mathbf{n}} = \nabla u$; the curvature, $\kappa = \nabla \cdot \hat{\mathbf{n}}$ and the velocity, $v = \partial u / \partial t$. We solve the equations in the sharp interface limit, when the profile of the interface is approximated as a step function. We assume that the precipitates correspond to $c = -C_e$ and the background to $c = +C_e$. The surface tension is σ . Let $\theta(u)$ represent the step function such that the profile is given by $c(u) = C_e [2\theta(u) - 1]$. The derivatives of c are given by $\nabla c = (\Delta C_e) \delta(u) \hat{\mathbf{n}}$ and $\dot{c} = (\Delta C_e) \delta(u) v$.

The normal coordinate u can be written as $u = r - r(a, t)$, where $r(a, t)$ describes the radial distance of the element a of the interface from the center of mass of the domain, and $v = -\dot{r}(a, t)$. In the sharp interface limit, the first part of the energy can be reduced to the drumhead Hamiltonian:

$$\int d\mathbf{r} \left[f(c) + \frac{1}{2} (\nabla c)^2 \right] \equiv \sigma \int da. \quad (\text{A5})$$

We start with the equation of motion

$$\frac{\partial c(\mathbf{r}, t)}{\partial t} = \nabla^2 \frac{\delta F(c)}{\delta c} + \xi(\mathbf{r}, t), \quad (\text{A6})$$

and define

$$P(\dot{c}) = -\frac{1}{2} \int \dot{c}(\mathbf{r}) \frac{1}{\nabla^2} \dot{c}(\mathbf{r}) d\mathbf{r} \quad (\text{A7})$$

such that the equation of motion becomes

$$\frac{\delta F(c)}{\delta c} + \frac{\delta P(\dot{c})}{\delta \dot{c}} = -\frac{1}{\nabla^2} \xi(\mathbf{r}, t). \quad (\text{A8})$$

We can define a new quantity,

$$\bar{F}(c, t) = F(c) + \int c(\mathbf{r}, t) h(\mathbf{r}, t) d\mathbf{r} \quad (\text{A9})$$

such that

$$\frac{\delta \bar{F}}{\delta c} = \frac{\delta F}{\delta c} + h \quad (\text{A10})$$

where $h(\mathbf{r}, t)$ is a field that accounts for the indeterminacy in the inverse Laplace operator and satisfies $\nabla^2 h(\mathbf{r}, t) = 0$. For periodic boundary conditions, it can be shown that h is only a function of t and the conservation law imposes the further condition $h(t) > 0$ [15]. In the sharp wall approximation, $\bar{F}(c)$ becomes

$$\begin{aligned} \bar{F}(c) &= \sigma \int da + h(t) \int c(u) dr \\ &- g_c \sum_{i,j} \int d\mathbf{r} d\mathbf{r}' d\mathbf{r}'' M_{ij}(\mathbf{r}, \mathbf{r}') M_{ij}(\mathbf{r}', \mathbf{r}'') \\ &\times c(u) c(u') c(u'') \end{aligned} \quad (\text{A11})$$

and

$$P = -\frac{(\Delta C_e)^2}{2} \int da da' v(a) G(\mathbf{r}(a), \mathbf{r}(a')) v(a'). \quad (\text{A12})$$

If there is a small displacement of the interface at a , $\delta\eta(a)$, the corresponding change in the concentration is $\delta c(\mathbf{r}) = (\Delta C_e)\delta(u(\mathbf{r})) \delta\eta(a)$ such that $\frac{\delta c(\mathbf{r})}{\delta\eta(a)} = \frac{\delta c(\mathbf{r})}{\delta v(a)} = (\Delta C_e)\delta(u(\mathbf{r}))$. The equation of motion becomes

$$\frac{\delta \bar{F}}{\delta\eta(a)} + \frac{\delta P}{\delta v(a)} = -(\Delta C_e) \int G(\mathbf{r}(a), \mathbf{r}') \xi(\mathbf{r}', t) d\mathbf{r}'. \quad (\text{A13})$$

We call Ω all the space and D the precipitate domains, such that $\Omega - D$ is the region occupied by the matrix. The elastic part of Eq. (A13) is

$$\begin{aligned} \frac{\delta \bar{F}_{el}}{\delta\eta(a)} &= -(\Delta C_e)g_c \sum_{ij} \int_{\Omega} d\mathbf{r}' \int_{\Omega} d\mathbf{r}'' \left[2M_{ij}(\mathbf{r}(a), \mathbf{r}') \right. \\ &\times M_{ij}(\mathbf{r}', \mathbf{r}'') + M_{ij}(\mathbf{r}(a), \mathbf{r}') \\ &\left. \times M_{ij}(\mathbf{r}(a), \mathbf{r}'') \right] c(u')c(u''). \end{aligned} \quad (\text{A14})$$

We design with T any of the integrals in the double integral above. Thus the double integral running over all space can be represented as $T_{\Omega}T_{\Omega}$ and it can be decomposed in three terms:

$$T_{\Omega}T_{\Omega} = T_D T_D + T_{\Omega-D} T_{\Omega-D} - 2T_D T_{\Omega-D}. \quad (\text{A15})$$

The first term above can be written as

$$\mu_{ij} = \begin{cases} \frac{\delta_{ij}}{d} \text{Tr}(\mu), & |\mathbf{r} - \mathbf{r}_A| < R_A \\ -\frac{R_A^d}{d} \text{Tr}(\mu) \left(\frac{d \mathbf{x}_{Ai} \mathbf{x}_{Aj} - r_A^2 \delta_{ij}}{r_A^{d+2}} \right), & r_A = |\mathbf{r} - \mathbf{r}_A| > R_A. \end{cases} \quad (\text{A20})$$

After some algebra, and assuming that two-body interactions are much stronger than higher-order interactions, Eq. (A16) can be written as

$$I_D(i) = \frac{d-1}{d} \sum_{j \neq i} \left(\frac{R_j^{2d} + 2R_i^d R_j^d}{|\mathbf{r}_i - \mathbf{r}_j|^{2d}} \right). \quad (\text{A21})$$

Because the shear strain is zero inside the precipitate, the "self-term," i.e., the term corresponding to the elastic en-

$$\begin{aligned} T_D T_D(\mathbf{r}(a)) &= \sum_{ij} \int_D d\mathbf{r}' \int_D d\mathbf{r}'' \left[2M_{ij}(\mathbf{r}(a), \mathbf{r}') \right. \\ &\times M_{ij}(\mathbf{r}', \mathbf{r}'') + M_{ij}(\mathbf{r}(a), \mathbf{r}') \\ &\left. \times M_{ij}(\mathbf{r}(a), \mathbf{r}'') \right] \end{aligned} \quad (\text{A16})$$

and similarly for the other two terms. We assume translational invariance of the tensor M_{ij} over the space Ω and take into account that $\sum_i M_{ii} = 0$. This means that $T_D T_{\Omega-D} = -T_D T_D$ and $T_{\Omega-D} T_{\Omega-D} = T_D T_D + \gamma$, where γ is an irrelevant constant related to the integration of the M_{ij} 's over all space [Eq. (A17) below means that the Laplacian is acting on $T_{\Omega}T_{\Omega}$]. Thus Eq. (A15) reduces to $T_{\Omega}T_{\Omega} = 4T_D T_D$. For simplicity, we call $T_D T_D = I_D$. The solution to Eq. (A13) is

$$\begin{aligned} (\Delta C_e)^2 \int G(\mathbf{r}(a), \mathbf{r}(a')) v(a') da' \\ = -\kappa(a)\sigma + (\Delta C_e)h(t) - 4(\Delta C_e)C_e^2 g_c I_D(\mathbf{r}(a)), \end{aligned} \quad (\text{A17})$$

where we have set the noise to zero. With the convention we have used, $\kappa(a) > 0$ when the center of curvature is in the domain [in particular, for a spherical domain of radius R , $\kappa = (d-1)/R$ and the critical radius is $R_c = (d-1)\sigma/(\Delta C_e)h(t)$].

The velocity equation can then be rewritten as

$$\int G(\mathbf{r}(a), \mathbf{r}(a')) v(a') da' = \frac{\sigma(d-1)}{(\Delta C_e)^2} \left[\frac{1}{R_c} - \frac{1}{r(a)} \right] - (\Delta C_e)g_c I_D(\mathbf{r}(a)), \quad (\text{A18})$$

where R_c is interpreted as an average critical size and $1/r(a)$ as a mean curvature.

This equation can be computed for spherical precipitates. Spherical precipitates have the property that the shear strain is zero inside them. Using Eq. (32) we write

$$\mu_{ij} - \frac{1}{d} \delta_{ij} \text{Tr}(\mu) = - \left(\frac{\partial^2 W}{\partial x_j \partial x_i} - \frac{\delta_{ij}}{d} c \right). \quad (\text{A19})$$

For a spherical precipitate centered at A

ergy evaluated inside the domain, and which is independent of the coordinates of precipitates, vanishes. Thus we are left only with the interaction term among precipitates. In particular, assume two three-dimensional(3D) spherical precipitates, A and B . Equation (A18) can be written as

$$R_A \dot{R}_A + \frac{R_B^2 \dot{R}_B}{r_{AB}} = 2 \left[\frac{1}{R_c} - \frac{1}{R_A} - \frac{2g_c R_B^3 (R_B^3 + 2R_A^3)}{3 r_{AB}^6} \right], \quad (\text{A22})$$

where $r_{AB} = |\mathbf{r}_A - \mathbf{r}_B|$ and we have made $(\Delta C_e) = 2$ and $\sigma = 4$. There is another equation with the indices A and B exchanged. We can assume sharp profiles so that all the concentration is inside the droplets. The conservation law requires

$$R_A^2 \dot{R}_A + R_B^2 \dot{R}_B = 0. \quad (\text{A23})$$

The velocity equation for the precipitate A can be rewritten as

$$R_A \dot{R}_A \left(1 - \frac{R_A}{r_{AB}}\right) = (R_A - R_B) \mathcal{C}(R_A, R_B, r_{AB}), \quad (\text{A24})$$

where

$$\mathcal{C}(R_A, R_B, r_{AB}) = \frac{1}{(R_A + R_B)} \left[\frac{1}{R_A} - \frac{1}{r_{AB}} + \frac{2}{3} g_c \frac{R_B (R_A^3 + R_B^3) (R_A^2 + R_A R_B + R_B^2)}{r_{AB}^6} \right] > 0. \quad (\text{A25})$$

Assume $R_A > R_B$. Equation (A24) implies that A will grow and B will shrink at a greater rate than that of Lifshitz and Slyozov. These are the results obtained by Kawasaki and Ohta in their statistical theory of Ostwald ripening with elastic field interactions. In their study they conclude that if the precipitates are hard, growth accelerates and if the precipitates are soft (i.e., $g_c < 0$), growth slows down. However, the assumption of soft precipitates is not good since the soft phase always deforms and wraps the hard domains. These equations are in strong contradiction with our simulations. We have simulated two precipitates of different radii with model B dynamics. Our simulations indicate that, in spite of having different radii, growth does not accelerate; quite the contrary, it finally stops. The above equations, however, clearly predict that the bigger domain will grow at the expense of the smaller one. It could be argued that deviations of the spherical shape could produce a nonvanishing self-term (since shear strain would be nonzero inside the precipitate) in the interface equations and thus account for the slow down. However, in our simulations we have put the two spherical precipitates at certain distance from each other and the deviations from the circular shape are completely negligible, i.e., the approximation of spherical precipitates is good, but still growth stops. We believe Eq. (A18) should be evaluated not at the interface but at a surface where the chemical potential is maximum.

We can generalize these equations for a model C system. Since the concentration is conserved, we expect it to be the slow variable governing the late-stage dynamics. If the precipitate is the ordered phase, i.e., $m_c = 0$, the elastic energy affects the concentration indirectly, through the order parameter.

The Eshelby interaction

$$f_E = [m_c(c - c_0) + m_y y^2] \sum_{i,j} \left[\left(\frac{\partial^2 W}{\partial x_j \partial x_i} - \frac{\delta_{ij}}{d} \nabla^2 W \right) \right]^2, \quad (\text{A26})$$

with

$$\nabla^2 W = \epsilon_c(c - c_0) + \epsilon_y y^2$$

can be rewritten, for the late stages, solely in terms of the

concentration, using the equilibrium condition $c + y^2 - 1 = 0$. By defining $\Delta\epsilon = \epsilon_y - \epsilon_c$ and $\Delta\mu = \mu_y - \mu_c$, we can rewrite W as

$$W = (\epsilon_y - \epsilon_c c_0) r^2 / (2d) - \nabla^{-2}(\Delta\epsilon) c$$

and

$$\frac{\partial^2 W}{\partial x_j \partial x_i} - \frac{\delta_{ij}}{d} \nabla^2 W = -(\epsilon_y - \epsilon_c) \left[\frac{\partial^2 W_c}{\partial x_j \partial x_i} - \frac{\delta_{ij}}{d} c \right], \quad (\text{A27})$$

where $\nabla^2 W_c = c$. Thus the energy can be written as

$$f_E = (m_y - m_c c_0) (\Delta\epsilon)^2 (1 - 1/d) c^2 + f_E^c, \quad (\text{A28})$$

$$f_E^c = -(\Delta\epsilon)^2 (\Delta\mu) c \sum_{i,j} \left[\frac{\partial^2 W_c}{\partial x_j \partial x_i} - \frac{\delta_{ij}}{d} c \right]^2.$$

f_E^c contains all the late-stage elastic effects that will modify the equation of velocity for c .

Thus we can write the velocity equation (A18) with $(\Delta C_e) = 1$ as

$$\int G(\mathbf{r}(a), \mathbf{r}(a')) v(a') da' = \sigma(d-1) \left[\frac{1}{R_c} - \frac{1}{r(a)} \right] - (\Delta\epsilon)^2 (\Delta\mu) I_D \left(\mathbf{r}(a) \right), \quad (\text{A29})$$

where as before R_c is interpreted as an average critical size and $\frac{1}{r(a)}$ as the mean curvature of the domain, and where $\sigma = \sigma_{1,0} = \sigma_{-1,0}$. Since the ordered domains form the hard phase, $\Delta\mu > 0$ (in our particular case $\Delta\mu = m_y$).

The case where the hard precipitate is the disordered phase is more delicate since there are competing effects between the tendency of the disordered phase to form the wetting layer along the ordered domains and the tendency to form circular domains due to the elastic forces. Particularly, in the late stage, when the disordered domains are already independent clusters, part of their interfaces are in contact with one sign of the ordered phase, and part with the other sign. Since $\sigma_{1,0} = \sigma_{-1,0}$ and

$c = 1 - y^2$ this distinction in signs may not be as crucial for the hard disordered domain and one could proceed as before, at least as a first approximation.

In this case, the sharp wall approximation for the concentration gives $c = \theta(-u)$, $\nabla c = -\delta(u)\hat{n}$, and $\dot{c} = -\delta(u)v$. For a small displacement of the interface at a , $\delta\eta(a)$, the corresponding change in the concentration is $\delta c(\mathbf{r}) = -\delta(u(\mathbf{r}))\delta\eta(a)$. This means that the elastic part of the chemical potential becomes $+(\Delta\epsilon)^2(\Delta\mu)I_D(\mathbf{r}(a))$,

but in this case $\Delta\mu < 0$ (in particular, $\Delta\mu = -m_c$), and so we can write the resulting equation of velocity for both cases as

$$\int G(\mathbf{r}(a), \mathbf{r}(a')) v(a') da' = \sigma(d-1) \left[\frac{1}{R_c} - \frac{1}{r(a)} \right] - (\Delta\epsilon)^2 \Delta\mu I_D(\mathbf{r}(a)). \quad (\text{A30})$$

-
- [1] A. G. Khachaturyan, *Theory of Structural Transformations in Solids* (John Wiley & Sons, New York, 1983).
- [2] A. J. Ardell, R. B. Nicholson, and J. D. Eshelby, *Acta Metall.* **14**, 1295 (1966).
- [3] See, for example, W. C. Johnson, *Acta Metall.* **32**, 465 (1984), and references therein.
- [4] J. W. Cahn, *Acta Metall.* **9**, 795 (1961).
- [5] K. Kawasaki and Y. Enomoto, *Physica A* **150**, 463 (1988).
- [6] W. C. Johnson and P. W. Voorhees, *Metall. Trans. A* **16**, 337 (1985).
- [7] A. Onuki, *J. Phys. Soc. Jpn.* **58**, 3065 (1989); **58**, 3069 (1989); H. Nishimori and A. Onuki, *Phys. Rev. B* **42**, 980 (1990); A. Onuki and H. Nishimori, *J. Phys. Soc. Jpn.* **60**, 1 (1990); A. Onuki and H. Nishimori, *Phys. Rev. B* **43**, 13649 (1991); H. Nishimori and A. Onuki, *J. Phys. Soc. Jpn.* **60**, 1208 (1991).
- [8] A. J. Bradley and A. H. Jay, *Proc. R. Soc. London, Ser. A* **136**, 210 (1932).
- [9] S. M. Allen and J. W. Cahn, *Acta Metall.* **23**, 1017 (1975); **24**, 425 (1976).
- [10] A. M. Somoza, C. Sagui, and R.C. Desai (unpublished).
- [11] L. D. Landau and E. M. Lifshitz, *Theory of Elasticity* (Addison-Wesley, Reading, MA, 1986).
- [12] E. D. Siggia and D. R. Nelson, *Phys. Rev. B* **15**, 1427 (1977); P. C. Hohenberg and D. R. Nelson, *ibid.* **20**, 2665 (1979); M. San Miguel and J. D. Gunton, *ibid.* **23**, 2317 (1981); M. San Miguel, J. D. Gunton, G. Dee, and P. S. Sahni, *ibid.* **23**, 2334 (1981); A. Chakrabarti, J. B. Collins, and J. D. Gunton, *ibid.* **38**, 6894 (1988).
- [13] Notice that the shear part of the elastic energy is $\int d\mathbf{r} \mu_0 \sum_{i,j} (\mu_{ij} - \frac{\delta_{ij}}{d} \nabla \cdot \mathbf{u})^2 = \frac{\mu_0}{k_{t0}^2} (1 - \frac{1}{d}) \int d\mathbf{r} [\epsilon_c(c - c_0) + \epsilon_v y^2]^2$, so that this expression together with the one coming from the compression term and the one coming from the coupling term give exactly $-\frac{1}{2k_{t0}} \int d\mathbf{r} [\epsilon_c(c - c_0) + \epsilon_v y^2]^2$.
- [14] For both model B and model C (and in general when there is a conserved concentration) the configurations depend on the mean concentration, c_0 . If the concentrations of the two phases are c_a and c_b , one can define a normalized concentration, $\chi = \frac{2c_0 - (c_a + c_b)}{c_b - c_a}$. Thus for our quenches with $c_0 = 1/3$ and $c_0 = 2/3$ we get the normalized concentrations $\chi = -1/3$ and $\chi = +1/3$.
- [15] K. Kawasaki and T. Ohta, *Physica A* **118**, 175 (1983); T. Ohta, *J. Phys. Condens. Matter* **2**, 9685 (1990).

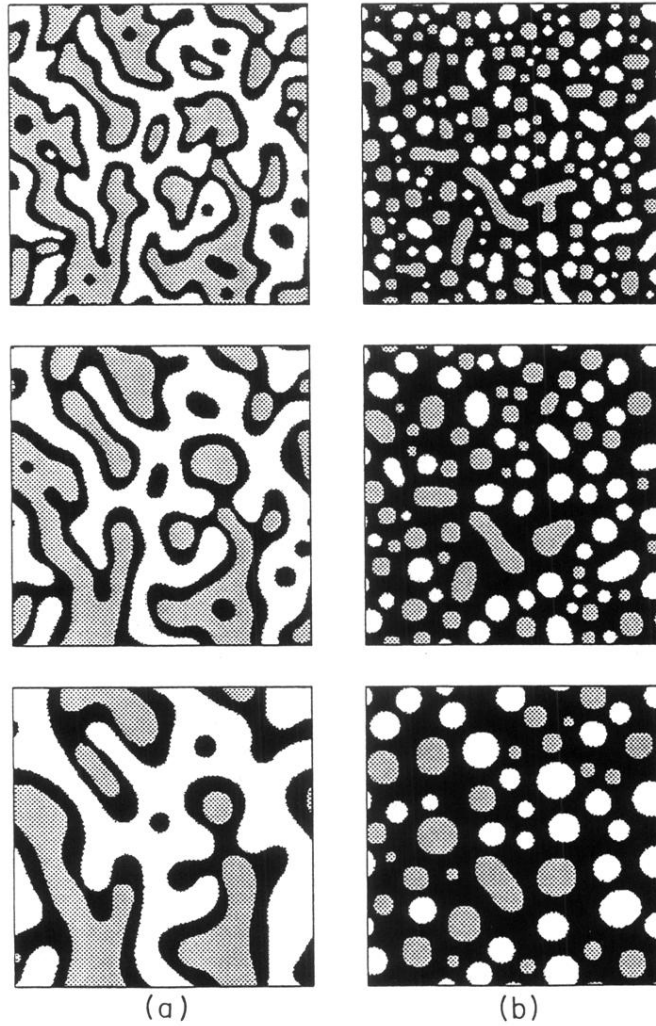


FIG. 2. Typical configurations for a model C system quenched into the order-disorder coexistence region, and with parameters chosen such that the disordered phase (black) forms a wetting layer that wraps the ordered domains with opposite sign (white or gray). The times shown in the picture correspond to $\tau = 150$, $\tau = 450$, and $\tau = 1500$, from top to bottom. (a) shows a quench with $c_0 = 1/3$ and (b) shows a quench with $c_0 = 2/3$.

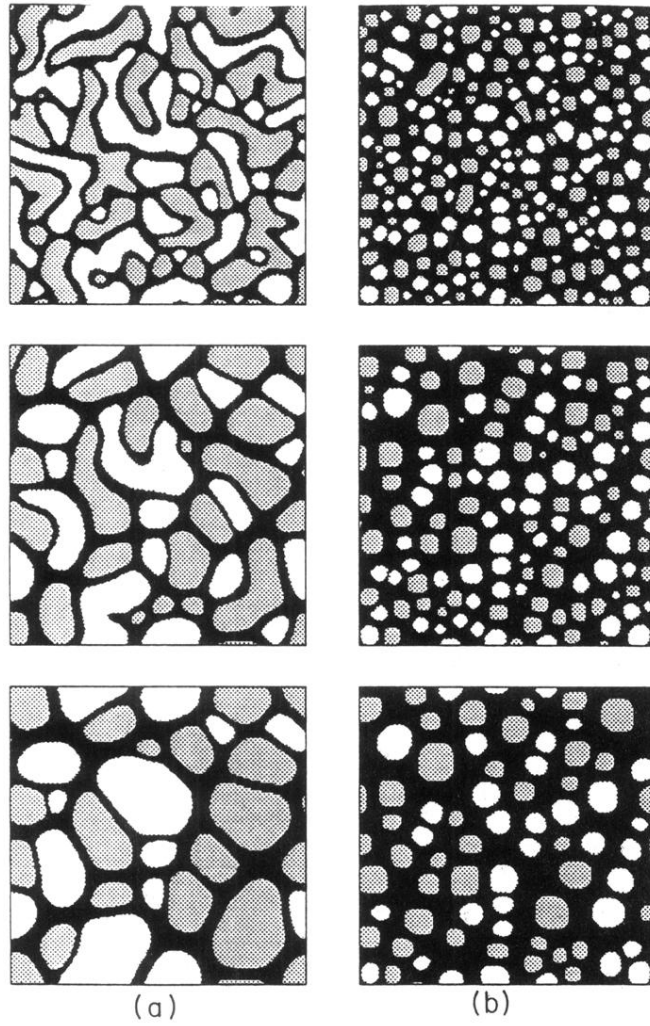


FIG. 3. Configurations where the ordered phase is the hard phase. (a) shows run A ($c_0 = 1/3$) and (b) shows run B ($c_0 = 2/3$). Times correspond to $\tau = 300, 1500,$ and $6000,$ from top to bottom.

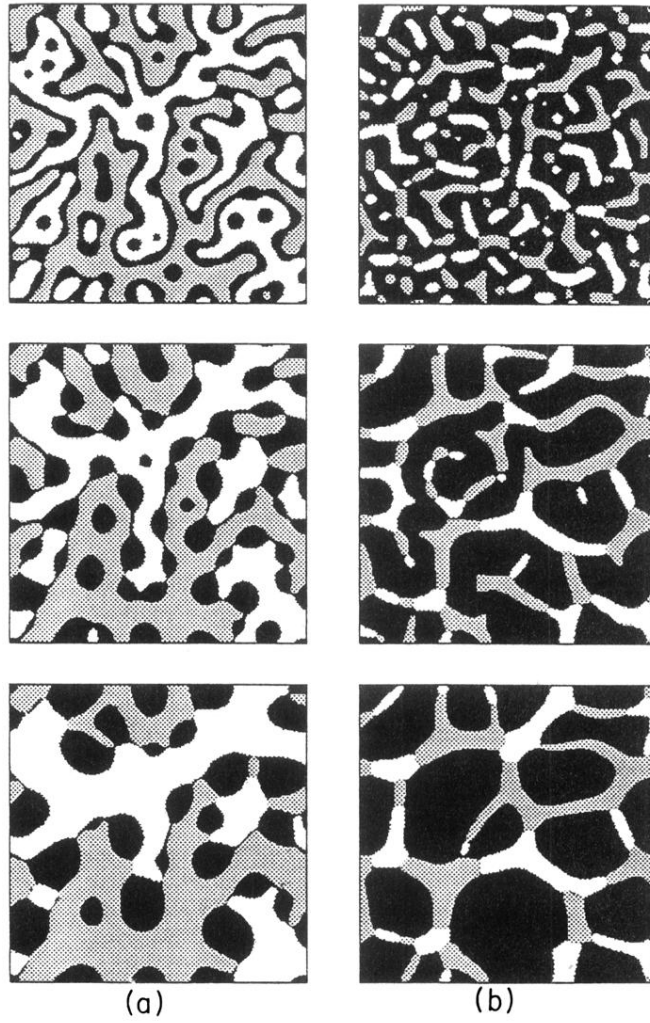


FIG. 4. Configurations where the disordered phase is the hard phase. (a) shows run C ($c_0 = 1/3$) and (b) shows run D ($c_0 = 2/3$). Times correspond to $\tau = 300, 1500,$ and 6000 , from top to bottom.

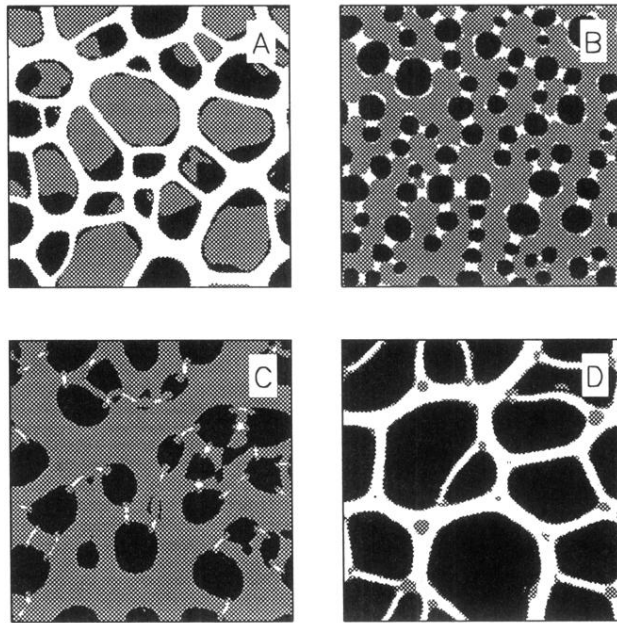


FIG. 6. Functional derivative of the elastic energy with respect to the concentration, $g = \delta F_{el} / \delta c$. The figures correspond to $\tau = 6000$, i.e., the last configurations shown in Figs. 3 and 4. The color scale is the following: white, $g > 0.2$; gray, $0 \leq g \leq 0.2$; black, $g < 0$.